Journal of Applied Polymer Science

Synthesis of lysozyme imprinted column with macroporous structure and enhanced selectivity: Utilization of cryogelation technique and electrostatic functional monomers

Seyed Mohammad Reza Kashefi Mofrad,[1] Fereshteh Naeimpoor,[1] Parisa Hejazi,[1] Ali Nematollahzadeh[2]

[1]Biotechnology Research Laboratory, School of Chemical Engineering, Iran University of Science and Technology, P.O. Box 16846-13114, Tehran, Iran

[2]Chemical Engineering Department, University of Mohaghegh Ardabili, Ardabil, Iran

Correspondence to: F. Naeimpoor (E-mail: fnaeim@iust.ac.ir)

ABSTRACT: Applicability of molecularly imprinted polymers (MIP) in conventional protein separation processes demands monolithic construction of columns with macroporous structure in addition to the high specificity and adsorption capacity. In this study, therefore, lysozyme (Lyz) imprinted monolithic cryogel columns were synthesized using electrostatic functional monomers (EFMs) to provide strong interactions between template and polymer, leading to specific recognition and capture of Lyz. SEM images and FTIR spectroscopy analysis confirmed the macroporous structure and presence of EFMs in the samples. Adsorption isotherms, heterogeneity, and breakthrough curves as well as selectivity of the molecularly imprinted cryogels (EFMs-MIC) and non-imprinted cryogels (EFMs-NIC) were investigated. Results showed effective imprinting with a maximum adsorption capacity of 211 mg/g and a high imprinting factor (IF) of 4.2 at low Lyz concentrations. A high relative selectivity coefficient of 7.24 was obtained for Lyz over cytochrome *c*, a competing protein, indicating that the imprinted sites could well distinguish Lyz. Reusability of MICs was also examined, where insignificant changes were observed in the cryogel adsorption/desorption characteristics after four cycles. Therefore, it is suggested to use EFMs and cryogelation in the synthesis of imprinted monolithic cryogels column for application in conventional protein separation processes. © 2015 Wiley Periodicals, Inc. J. Appl. Polym. Sci. **2016**, *133*, 42880.

KEYWORDS: adsorption; gels; molecular recognition; porous materials; proteins

Received 19 May 2015; accepted 26 August 2015
DOI: 10.1002/app.42880

INTRODUCTION

Separation and purification of proteins, a group of important biologically active molecules with diverse applications in medicine, have been the focus of many researches in the last decades. Among various methods, molecular imprinting technique has recently been used in separation and recognition of proteins by molding the template molecules in a polymeric matrix. After removing the template from polymer, the resulted cavities can be employed to specifically isolate and recognize the template molecule from a mixture.[1]

Molecularly imprinted polymers (MIPs) can well be used in separation processes such as high performance liquid chromatography (HPLC), solid phase extraction (SPE), and capillary electro-chromatography (CEC) in the form of either packed or monolithic columns.[2] The latter form however is preferred because of the one step synthesis procedure,[3] diffusional and hydrodynamic benefits as well as their high performance.[4] To synthesize imprinted columns with macroporous structure at much lesser expense, cryogelation can be exploited in which polymerization process takes place at low temperatures around −14 to −18°C.[5–7] Molecularly imprinted cryogel (MIC) monolithic columns based on acrylate chemistry and free radical crosslinking polymerization in aqueous solutions[8] have so far been fabricated for recognition of several molecules such as pollutants, bilirubin, L-glutamic acid, bisphenol A, 17β-estradiol, lysozyme (Lyz), and etc.[9–15] Although MIPs/MICs have been successfully used for small molecules,[16,17] imprinting of macromolecules such as proteins has been associated with challenges due to their large size, structural change or insolubility in polymerization medium as well as diffusional restrictions.[18,19] Nonetheless, imprinting of a number of proteins has been carried out through bulk (3D), surface (2D), and epitope techniques.[20,21]

Despite the fact that acrylate chemistry due to its water compatibility has been frequently used in the synthesis of imprinted

polymers,[22] water, and other similar molecules (forming hydrogen bonding) compete with proteins to enter the created sites in aqueous solvents and this adversely affects the imprinting factor. To alleviate this problem, template molecules are firstly mixed with electrostatic functional monomers (EFMs) such as methacrylic acid (MAA) and 2-dimethyl amino ethyl methacrylate (DMA) in a pre-polymerization process, where powerful electrostatic interactions result in the formation of complexes between functional groups on template (protein) surface and EFMs.[23–25] During imprinting stage hence the electrostatically bound EFMs take part in polymerization and molding process, providing more specific sites. To study formation of these complexes, UV difference spectroscopy technique has been used by some researchers, where the difference between absorbencies of a mixture consisting of EFMs in addition to template molecules and its individual components is taken as a measure of the formed complexes. Complex formation between di-peptide and MAA,[26] Lyz and acrylamide (AAm),[27] and bovine hemoglobin and AAm[28] as well as MAA and DMA with Lyz[29] has so far been studied. Earlier applications of EFMs were based on equal amounts of EFMs alongside AAm as neutral-hydrophilic monomer.[24,25,30,31] Later to account the type and amount of EFMs in Lyz imprinting process, Bergmann exploited EFMs (MAA and DMA) at a theoretical ratio equal to the corresponding positively (lysine, arginine, and histidine) to negatively (aspartic and glutamic acids) charged amino acids on Lyz surface,[32] which improved imprinting effect compared to equal amounts of EFMs. Recently, saturation interaction study of EFMs with Lyz molecules has shown that the saturation ratio of EFMs at the lowest free amounts of EFMs well works for specific recognition of Lyz by imprinted hydrogels synthesized by bulk method.[29] It should however be mentioned that these synthesized hydrogels need to be crushed before use and this partly destroys the specific sites and hence reduces the imprinting effect. This necessitates synthesizing Lyz imprinted monolithic cryogels providing macroporous structure beneficial in practical separation applications.

MATERIALS AND METHODS

Materials

Acrylamide (AAm), methacrylic acid (MAA), and 2-dimethyl amino ethyl methacrylate (DMA) as functional monomers, *N,N′*-methylene bisacrylamide (MBA) as crosslinker, ammonium persulfate (APS), and *N,N,N′,N′*-tetra methyl ethylene diamine (TEMED) as initiator system, lysozyme from hen egg white source as template and cytochrome *c* (Cyt *c*) from equine heart as competitor protein were purchased from Sigma-Aldrich.

EXPERIMENTS

Synthesis of EFMs-MIC(NIC)

To synthesize EFMs-MIC (Lyz imprinted cryogel containing EFMs) samples, complex formation between Lyz and functional monomers was carried out in the first stage by using Lyz and EFMs (DMA and MAA) at amounts based on saturation interaction of EFMs and the minimum free to total EFMs ratio for Lyz imprinted hydrogel.[29] AAm was used as structural functional monomer at an amount calculated based on the total monomer previously used for Lyz imprinted cryogel.[33] Bulk polymerization was then carried out by addition of crosslinker: MBA, accelerator: TEMED, and initiator: APS at low temperature to prepare soft monolithic cryogels columns.

Separate stock solutions of AAm (312.5 mg/mL), EFMs: MAA (10.2 μL/mL), and DMA (9.26 μL/mL), MBA (17 mg/mL), proteins (50 mg/mL), all in sodium phosphate buffer (SPB, 10 m*M*, pH=7.0) as well as stock solutions of initiator system: APS (10 mg/mL) and accelerator: TEMED (30 μl/mL) in double distilled water (kept at 4°C) were prepared and an appropriate amount of each solution was used when required. Complex formation was carried out by addition of AAm: 88.13 mg, MAA: 1.30 μl, DMA: 0.59 μl, and template, Lyz: 3.75 mg into a glass vial and keeping the solution for 20 min. Subsequently, MBA, 10 mg was added and after 3 min TEMED (3 μL per 1 mg APS) and APS (0.4% of total monomers) were added and the final mixture (1.25 mL) was gently shaken at ambient temperature.[29,33] Of this mixture, 1 mL was transferred into a glass tube which was sealed and kept in freezer to polymerize at -17 ± 1°C for 16 h.

Synthesized samples were then washed by pumping distilled water (DW) enormously to remove unreacted (free) monomers, soluble oligomers, and other substances. To release LYZ, the samples were washed with 50 mL of NaCl solution (0.5 *M* at a flow rate of 1.5–2 mL/min) and this was followed by pumping 100 mL of DW through the cryogel samples to remove the remaining salt.[24] Lyz concentration was determined by UV absorbency at 280 nm (CECIL Bio Quest). EFMs-NIC (non-imprinted cryogel containing EFMs) was synthesized in the same manner except in the absence of Lyz. All experiments were carried out in triplicate. Cryogels were thawed at room temperature and kept in distilled water before use.

Lyz Rebinding

Three EFMs-MIC samples each in a glass tube (volume of 1 mL) were lined up and 22 mL of Lyz solution (0.5 mg/mL of SPB) was recirculated through the samples at 1.5 mL/min and ambient temperature for about 25–30 min until reaching constant Lyz concentration. To determine Lyz adsorption capacity of the cryogels, UV absorbance of the solution was read at 280 nm and reported as the overall performance of the three cryogel samples.[34] EFMs-NIC samples were similarly treated.

Adsorption Isotherms

To obtain Lyz adsorption isotherms, Lyz solutions at initial concentrations (C_0) of 0.33 to 6.5 mg/mL in SPB (10 m*M*, pH 7.0) were prepared and sequentially recirculated through EFMs-cryogels (MIC and NIC) until reaching constant Lyz concentrations (equilibrium concentration: C_e, mg/mL) which were measured by a Cecil-Bioquest spectrophotometer.

Knowing C_0, C_e and the dry weight of cryogel, adsorption capacity (Q, mg adsorbed Lyz/g cryogel) was calculated and plotted versus C_e. Using nonlinear regression, these data were fitted into Langmuir and Freundlich equations[34] as given in eqs. (1) and (2), respectively, and their parameters were estimated.[34]

$$Q = \frac{Q_{max} K_a C_e}{1 + K_a C_e} \quad (1)$$

where Q_{max} is the maximum Lyz adsorption capacity (mg/g) and K_a is the association constant for Lyz to cryogels.

$$Q = K_f C_e^{\frac{1}{n}} \quad (2)$$

where K_f and n are Freundlich adsorption constant (mg/g) and exponent, respectively.

Additionally, Scatchard analysis[35] were performed to estimate Lyz association constants for high and low affinity domains. Having Q and C_e from rebinding experiments, Q/C_e was plotted versus Q leading to biphasic lines, wherein the slope of each line gives the corresponding association constant according to eq. (3):

$$\frac{Q}{C_e} = K_a Q_{max} - K_a Q \quad (3)$$

Lyz Removal and Cryogel Reusability

Lyz bound to the polymer matrix should be removed after the synthesis of imprinted samples and rebinding experiments to make cryogels usable/reusable for further experiments. This was carried out by passing 50 mL of DW followed by 100 mL of NaCl aqueous solution (0.5 *M*) through the cryogels placed in a glass tube at a flow rate of 1.0 mL/min for about 30 min. Lyz recovery from cryogels was then determined by measuring the final Lyz concentration in recovery solution.

To test the reusability, the same imprinted sample was taken to perform four cycle of adsorption–desorption experiments. After each adsorption experiment, Lyz was desorbed from the sample as mentioned above. The sample was then washed again with adequate amount of DW to remove the remaining salt and re-equilibrated with SPB solution before next adsorption experiment.

Adsorption Breakthrough Curve Analysis

Binding strength of an analyte to an absorbent is usually evaluated by continuous passing of the analyte solution through the sorbent column and plotting the breakthrough curve (i.e. the ratio of outlet to inlet analyte concentrations versus the volume passed). The volume corresponding to the observed sharp increase specifies the breakthrough volume.[36] Therefore, breakthrough behavior and volumes for MIC and NIC samples were obtained to compare binding strength of Lyz towards each sample. Breakthrough curve was also exploited to calculate the final amount of adsorbed Lyz (m_f) by each column using eq. (4):

$$m_f = C_0 . V_f - C_0 \int \frac{C}{C_0} dV \quad (4)$$

where C and C_0 are the outlet and inlet Lyz concentrations and V is the passed volume. V_f is the volume at which C/C_0 reaches unity and remains constant.

To obtain breakthrough curve, 100 mL of Lyz solution at 0.55 mg/mL was continuously pumped at a flow rate of 1 mL/min through three MIC (NIC) samples with total mass of 178.9 (196.9) mg lined in a column and Lyz concentration in solution was monitored over time.

ANALYSIS

Characterization of Cryogels

The morphology and structure of the dried EFMs-MIC and EFMs-NIC were characterized by scanning electron microscopy (SEM) and Fourier-transform infrared spectroscopy (FTIR). The sample was firstly fixed in 2.5% glutaraldehyde and 0.1*M* SPB (pH 7.0) overnight and then washed three times using the same buffer. This was followed by post-fixation in 1% osmium tetroxide for 1 h and re-washing. After dehydration by ethanol-water mixtures at 0, 25, 50, 75, and 99.5%, sample was transferred to a critical point drier and coated with gold–palladium (40 : 60). A cross section of the samples was examined using a model KYKY-EM3200 SEM.[37,38]

To identify presence of functional groups, FTIR analysis was carried out. FTIR spectra were recorded for the cryogel samples embedded in KBr pellets with a RX1 Spectrometer (Perkin–Elmer).

Swelling ratio of the cryogels was calculated by using dry and wet weights as given in eq. (5).[39] Cryogels were first dried at 60°C for at least 48 h until constant weight and then immersed in DW for 1 h to obtain the wet weight.

$$Swelling\ Ratio\ (SR) = \frac{(m_{wet} - m_{dry})}{m_{dry}} \quad (5)$$

m_{wet} and m_{dry} are the masses of swollen and dried cryogels, respectively.

To identify the portion of total monomers participating in polymerization reaction, gel fraction yield was calculated as given in eq. (6):[14]

$$Gel\ Fraction\ Yield\ (GFY) = \frac{m_{dry}}{m_{total\ \ monomers}} \quad (6)$$

where $m_{total\ \ monomers}$ is the total mass of monomers (AAm, MAA, and DMA) and crosslinker (MBA) used in cryogel synthesis.

Adsorption Capacity and Distribution Coefficient

Adsorption capacity (Q, mg/g) defined as the ratio of adsorbed protein (mg) to the dry mass of cryogel (g) was calculated for both EFMs-MIC and EFMs-NIC samples as given in eq. (7):

$$Q = \frac{(C_0 - C_e)}{m_{dry}} \times V \quad (7)$$

where C_0 and C_e are the initial and final concentrations of protein solution (mg/mL), V (mL) is the volume of rebinding solution and m_{dry} is the dry weight of cryogel (mg). Knowing Q and C_e, protein (Lyz or Cyt *c*) distribution coefficient (K_d, mL/g) in rebinding solution can be calculated using eq. (8):

$$K_d = \frac{Q}{C_e} \quad (8)$$

Imprinting factor (IF) was calculated using eq. (9):

$$IF = \frac{(K_d)_{MIC}}{(K_d)_{NIC}} \quad (9)$$

where $(K_d)_{MIC}$ and $(K_d)_{NIC}$ correspond to distribution coefficients of imprinted and non-imprinted cryogels, respectively.

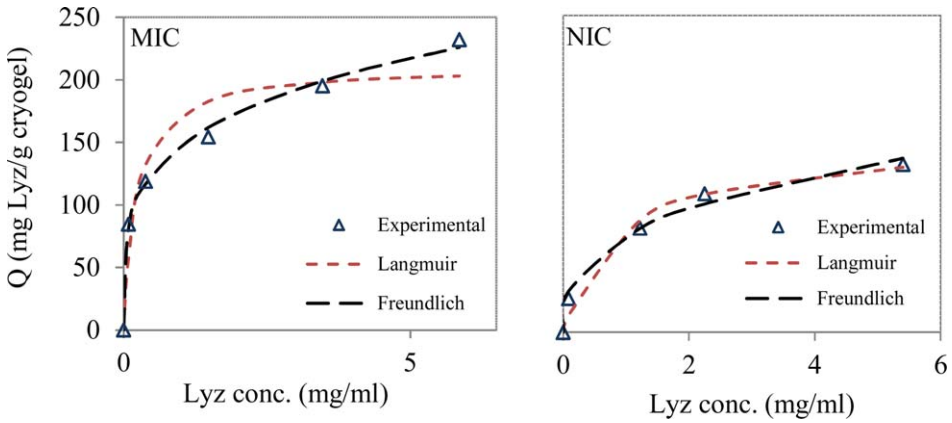

Figure 1. Adsorption isotherms for LYZ on EFMs-cryogels (MIC: left and NIC: right) and the corresponding Langmuir and Freundlich isotherms obtained based on nonlinear regression. [Color figure can be viewed in the online issue, which is available at wileyonlinelibrary.com.]

SELECTIVITY

Specificity of the synthesized samples toward Lyz adsorption was examined using Cyt *c* (*M*w= 12.3 KDa and isoelectric point of 10) as competitor due to its similarities to Lyz (*M*w= 14.6 kDa and isoelectric point of 11). SPB solution containing Lyz and Cyt *c* each at 0.5 mg/mL was recirculated through three lined samples until reaching equilibrium. Lyz and Cyt *c* adsorption onto the samples were determined by measuring the supernatant absorbance at 280 and 408 nm, respectively.[40,41] To assess the selective binding of Lyz with competing protein (Cyt *c*) and influence of imprinting, selectivity coefficient (k), and relative selectivity coefficient (k') were calculated as given in Eqs. (10) and (11), respectively.

$$k = \frac{K_d(LYZ)}{K_d(Cyt\ c)} \tag{10}$$

$$k' = \frac{k_{MIC}}{k_{NIC}} \tag{11}$$

RESULTS AND DISCUSSION

Adsorption Studies

Adsorption Isotherms. Equilibrium isotherms for Lyz adsorption on EFMs-cryogels (MIC and NIC) are shown in Figure 1. As can be seen, adsorption capacity sharply increases with concentration at lower range and its rate of change gradually decreases until capturing all the available binding sites, resulting in saturation condition. This behavior can well be expressed by Langmuir or Freundlich models as shown in Figure 1.

Using nonlinear regression, parameters of Langmuir and Freundlich isotherms for Lyz adsorption by EFM-MIC(NIC) were estimated as given in Table I. As can be seen, adsorption capacities (K_f in Freundlich and Q_{max} in Langmuir models) were higher for EFMs-MIC compared to EFMs-NIC samples, implying appropriate imprinting efficiencies. Adsorption capacities of Q_{max} = 211 and K_f = 147 mg/g obtained for EFMs-MIC in this work are much higher than those previously reported for Lyz adsorption by AAm-MIC (Q_{max} = 36.9 and K_f = 11.4 mg/g)[33] as well as by Lyz-imprinted polyacrylamide using silica (K_f = 30.75 mg/g).[42]

Table I also shows the suitability of Freundlich isotherm for our EFMs-MIC samples (R^2 for EFMs-MIC: 0.996 and EFMs-NIC: 0.99) as compared to the suitability of Langmuir isotherm for AAm-MIC samples (R^2 for AAm-MIC: 0.985 and AAm-NIC: 0.992).[33] This can be explained by the fact that Langmuir isotherm is based on monolayer adsorption on homogeneous surface with no interactions of adsorbed and free molecules which is more consistent with AAm cryogels. On the contrary, our cryogel samples containing EFMs show heterogeneity and hence can best be described by Freundlich isotherm which considers adsorption on a heterogeneous surface and interactions of adsorbed and free molecules.[43]

Using Scatchard analysis for EFMs-cryogels, Lyz association constants at high and low affinity sections, corresponding to the specific sites and nonspecific recognition parts, were obtained from the slope of the related lines as given in Figure 2 and Table II. Although similar association constants of 0.95 and 0.87

Table I. Parameters and Fitness of Langmuir and Freundlich Models for LYZ Adsorption by EFMs-Cryogels and AAm-Cryogels[33] (MIC: Imprinted and NIC: Non-Imprinted)

		Freundlich			Langmuir		
Cryogel Type		R^2	n	K_f (mg/g)	R^2	K_a (mL/mg)	Q_{max} (mg/g)
EFMs	MIC	0.996	4.13	147.2	0.924	4.381	211
	NIC	0.990	2.88	76.44	0.982	1.148	151.2
AAm	MIC	0.942	1.88	11.40	0.985	0.524	36.29
	NIC	0.969	1.69	7.58	0.992	0.801	18.22

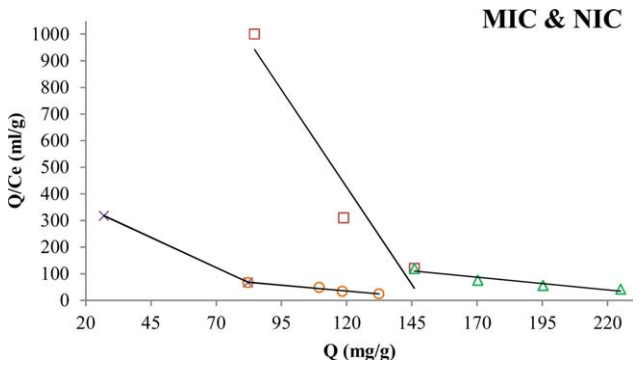

Figure 2. Scatchard plots for LYZ adsorption on EFMs-cryogels at 25°C, MIC (× high, ○ low affinities), and NIC (□ high, △ low affinities). [Color figure can be viewed in the online issue, which is available at wileyonlinelibrary.com.]

were obtained at low affinity regions for both MIC and NIC samples, the ratio of high to low affinity association constants of nearly 15 was obtained for EFMs-MIC, whereas this was about five for EFMs-NIC. Due to the strong affinity named as imprinting entity (Figure 2), the observed difference for EFM-MIC was much higher than that for EFM-NIC. Additionally, higher maximum binding capacities were obtained for EFMs-MIC compared to EFMs-NIC in either of high or low affinity region indicating the imprinting effect.

Table II. Estimated Parameters and Fitnesses (R^2) for Synthesized EFMs-Cryogels at High and Low Affinity Parts of Scatchard Plot Shown in Figure 2

Cryogel Type	Affinity[a]	K_a (mL/mg)	Q_{max} (mg/g)	R^2
MIC	H	14.62	149.1	0.938
	L	0.95	260.9	0.909
NIC	H	4.54	97.1	1.000
	L	0.87	160.6	0.976

[a] H: high and L: low affinity sections of biphasic curve.

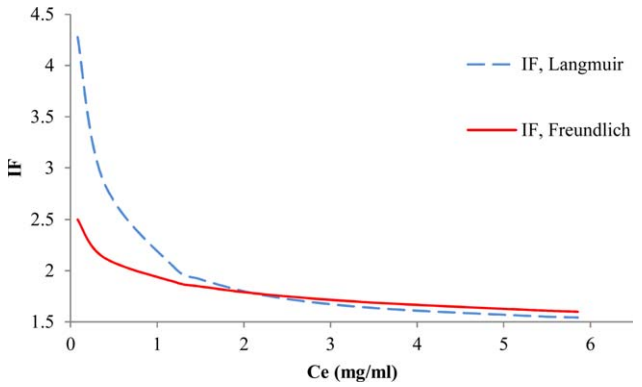

Figure 3. Imprinting factor of EFMs-cryogel based on Freundlich and Langmuir isotherms. [Color figure can be viewed in the online issue, which is available at wileyonlinelibrary.com.]

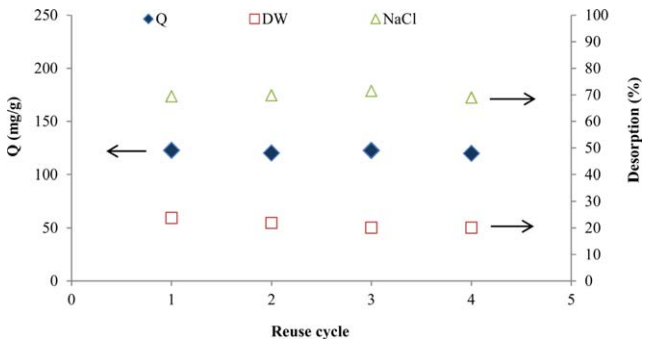

Figure 4. LYZ adsorption capacity as well as its desorption after passing distilled water (DW) and elution agent (NaCl) for EFMs-MIC during reuse. [Color figure can be viewed in the online issue, which is available at wileyonlinelibrary.com.]

The observed difference between the high and low affinity association constants for our EFM-NIC sample can be attributed to the heterogeneity caused by presence and uneven distribution of EFMs in the cryogel. In contrast, using AAm as sole functional monomer[33] resulted in similar association constants at low and high affinity regions, which is consistent with the homogenous structure of cryogel.

IMPRINTING FACTOR

Imprinting factor of EFMs-cryogel was calculated and plotted versus equilibrium Lyz concentration (C_e) based on Freundlich and Langmuir isotherms (see Figure 3).

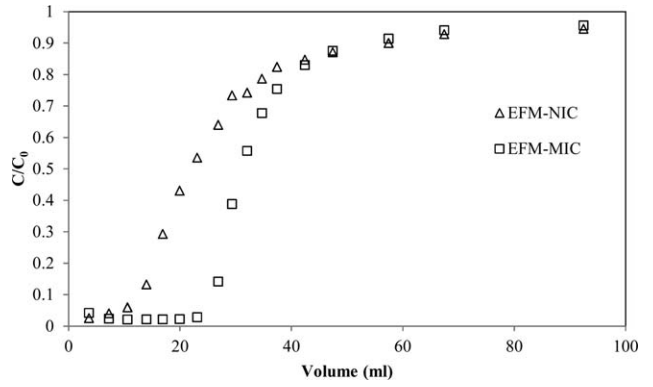

Figure 5. Breakthrough curves for imprinted (EFMs/MIC) and non-imprinted (EFMs-NIC) columns.

Table III. Swelling Ratios and Gel Fraction Yields of EFMs-Cryogels Compared with Those Previously Reported for AAm-Cryogels[33]

	Type of cryogel			
	EFMs		AAm	
Specifications	MIC	NIC	MIC	NIC
Swelling ratio	19.7	17.2	24.5	20.5
Gel fraction yield (%)	74.4	80.9	72	90

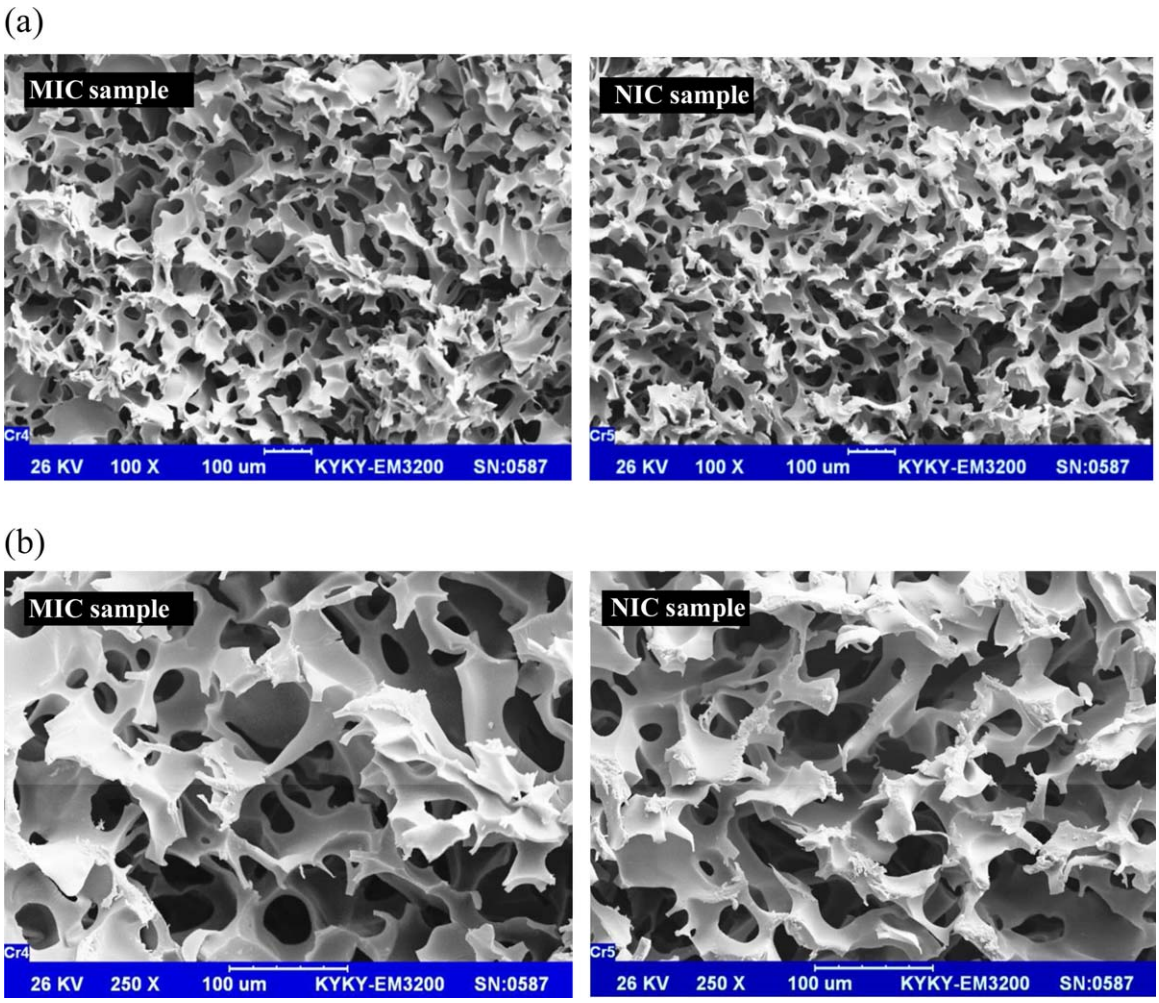

Figure 6. SEM images of EFMs-cryogels (MIC and NIC), (a) 100× magnification and (b) 250× magnification. [Color figure can be viewed in the online issue, which is available at wileyonlinelibrary.com.]

The highest imprinting factors for Langmuir (about 4.3) and Freundlich (2.5) isotherms correspond to the lowest value of C_e. This means the higher affinity of EFMs-MIC for Lyz at diluted solutions and confirms construction of specific recognition sites. Similar IF values were obtained for both isotherms at high C_e. Compared to AAM-cryogel,[33] the higher IF value obtained for EFMs-MIC in this study could be due to the more specific sites created by strong electrostatic interactions of EFMs (MMA and DMA) with Lyz.

Lyz Recovery and Reusability of EFMs-MIC

Since adsorbent recovery is one of the most important issues in separation processes, reusability of the synthesized EFMs-MIC was investigated by four times repetition of adsorption–desorption cycle using the same EFMs-MIC sample. Desorption stage in each cycle was accomplished using distilled water followed by NaCl solution as elution agent to differentiate weak and electrostatic bonds of Lyz with polymer, respectively. Figure 4 presents Lyz adsorption capacity as well as percentages of Lyz desorption after passing distilled water and NaCl solution in each reuse cycle.

Overall, a high Lyz desorption of about 92% was achieved in each cycle, of which about 20% corresponded to passing distilled water, showing nonspecific or weak bindings while passing elution agent resulted in 71% desorption by weakening electrostatic bonds between Lyz and polymer in more specific sites. Negligible change was observed in adsorption/desorption performance of imprinted cryogels over reuse.

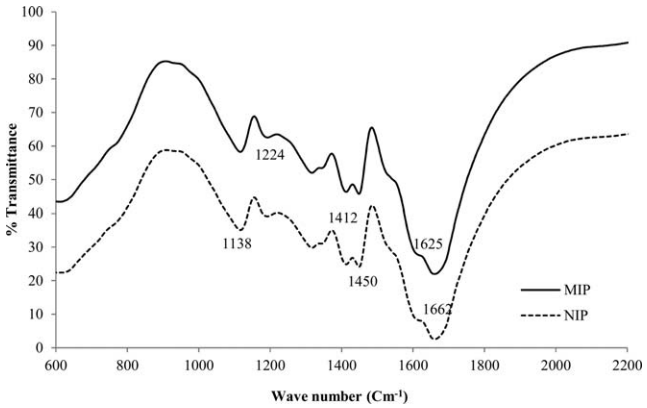

Figure 7. FTIR spectra of MIC and NIC samples.

Table IV. Results of Selectivity (of LYZ over Cyt c) Analysis for EFMs-Cryogels (MIC and NIC)

	EFMs-cryogels						
	MIC			NIC			
Protein	K_d (mL/g)	k	Q_{max} (mg/g)	K_d (mL/g)	k	Q_{max} (mg/g)	k′
LYZ	1129.6	8.7	74.1	141	1.2	37.1	7.24
Cyt c	129.7		37.2	117.1		33.7	

Breakthrough Behavior of EFMs-MIC/NIC Column

To show the affinity of EFMs-cryogels toward Lyz, breakthrough curves for MIC and NIC columns are presented in Figure 5.

Breakthrough volumes of 23 and 3 mL were obtained for MIC and NIC, respectively. This implied much stronger bonds between Lyz and MIC compared to NIC. Taking into account the higher mass of NIC (196.9 mg) compared to MIC (178.9 mg) intensifies the superiority of MIC over NIC with respect to Lyz adsorption. Additionally, the final amount of adsorbed Lyz (m_f) by MIC (NIC) column was calculated as 15.46 (11.71) mg, and considering the weight of column, saturation point of 86.4 (59.5) mg Lyz/g column was estimated. The higher saturation point for MIC column showed the specific Lyz adsorption capacity of MIC compared to NIC.

Characterization of Cryogels

As apparent, the synthesized EFMs-MIC and EFMs-NIC were white in color and spongy and swelled very fast after immersing in DW. A comparison of swelling ratios (SR) and gel fraction yields (GFY) of the synthesized samples with those previously reported for AAm-cryogels[33] is illustrated in Table III.

As expected for the two types of cryogels, MIC samples showed higher SR and lower gel fraction yield as compared to NIC. This can be attributed to the presence of giant LYZ molecules in MIC samples resulting in pore formation and partial disruption of polymer matrix, which obstructs complete polymerization. EFMs-cryogels, however, showed lower values of swelling ratio compared to AAm-cryogels possibly due to the formation of smaller macropores.[41] Higher gel fraction yields obtained for the synthesized imprinted and non-imprinted EFMs-cryogels compared to the previously reported[44] values of 70–80% can be attributed to the presence of EFMs within polymer matrix. Similarly, Derazshamshir and coworkers reported reduced gelation yield for poly(HEMA) cryogel imprinted by hemoglobin (Hb) compared to its non-imprinted sample.[34]

Table V. Comparison of rebinding properties of some imprinted cryogels

	Properties[a]			
Imprinted cryogel	K	k′	Q_{max}	Reference
EFMs	8.7	7.24	211	This study
AAm	-	1.37	36.29	33
Silica base	-	-	30.75	42
Carbon nanotube base	1.4	1.3	20.89	20
Cu^{2+}-coordinating monomer	6.19	3.2	22.9	13
L-Histidine imprinted	2.67	2.4	54.2	40

[a] Q_{max} (mg/g): maximum adsorption capacity, k: selectivity and k′: relative selectivity coefficients.

SEM And FTIR Analyses

Figure 6 shows SEM images of internal structures of MIC and its corresponding NIC samples. Both cryogels showed interconnected macroporous structure with thin polymer walls, which provide channels for easy access of the mobile phase to the created binding sites without significant mass transfer resistance. Macropores in scale of 5–100 μm distributed in the polymer network were much bigger than the elliptical LYZ molecule in size of 4.0 ×4.0 ×14.0 nm facilitating Lyz transfer through the cryogel.

FTIR spectra of MIC and NIC cryogels demonstrated in Figure 7 showed quite similar type and relative intensities of peaks for the entire spectrum range, showing that MIC and NIC samples were chemically alike and Lyz had insignificant impact on chemical structure of the cryogels. Presence of MAA was evidenced by strong absorption band at 1662 cm^{-1} (C=O stretch) and the peak at 1414 and 1450 cm^{-1} (O–H bending). C=O stretching peak and its shoulder peak at 1625 cm^{-1} (N–H bending) indicated the presence of AAm in copolymer. Presence of EFMs was confirmed by peaks at 1664 cm^{-1} (C=O), 1138 cm^{-1} (C–N stretch), and 1224 cm^{-1} (C–O stretch) for DMA.

Selectivity of EFMs-Cryogel

Competitive adsorption of Lyz by EFMs-cryogel was investigated using a solution containing Cyt *c* and Lyz (each at 0.5 mg/mL). Comparisons of K_d, *k*, and Q_{max} for MIC and NIC samples are demonstrated in Table IV. Although Q_{max} values for Cyt *c* were nearly similar for both samples, the maximum Lyz adsorption capacity of MIC was nearly two times that for NIC. Much higher value of K_d for Lyz (1129.6 mL/g) alongside the higher selectivity coefficient ($k = 8.7$) obtained for MIC confirms the specificity of the sites created during the imprinting process of Lyz. Taking into account that *k* value for NIC is 1.2, a relative selectivity coefficient of 7.24 for the template (Lyz) over a similar analyte (Cyt *c*) can be reported for the synthesized EFMs-MIC samples. It should also be mentioned that there was no major difference evidenced for pure Lyz and Cyt *c* adsorption test compared to competitive mixture.

Comparison of the rebinding properties achieved in this work with those previously reported on imprinted cryogels, given in

Table V, shows the high adsorption capacity and selectivity coefficients for our EFMs-cryogel sample. This evidences the effectiveness of this approach in formation of more specific imprinted sites alongside the high capacity and hence the superiority of EFMs-cryogel application in industrial separation processes.

CONCLUSIONS

In this study, we synthesized Lyz imprinted polymers using electrostatic functional monomers in combination with cryogelation technique to obtain macroporous imprinted monolithic cryogels and their physical and rebinding properties were examined. Macroporous structure and presence of electrostatic functional monomers in the synthesized cryogels were approved by SEM and FTIR spectroscopy analyses, respectively. Adsorption parameters estimated from experimental data revealed the superiority of EFMs-MIC samples with maximum adsorption capacity of 211 mg Lyz/g cryogel, relative selectivity coefficient of 7.24 for Lyz/Cyt *c* as compared to those previously reported for AAM-cryogels. Taking into account the similarities in morphology of the synthesized MIC and NIC as observed via SEM images, Lyz adsorption differences between MIC and NIC samples, and improved imprinting effect of EFMs-MIC, was concluded to be the result of the highly specific sites formed within the polymer matrix. It was finally shown that the monolithic EFMs-MIC columns could well be used in repeated cycles with insignificant changes in their performance. This novel approach can have generic application in enhanced separation of other biological macromolecules.

REFERENCES

1. Mahony, J. O.; Nolan, K.; Smyth, M. R.; Mizaikoff, B. *Anal. Chim. Acta.* **2005**, *534*, 31.
2. Vasapollo, G.; Sole, R. D.; Mergola, L.; Lazzoi, M. R.; Scardino, A.; Scorrano, S.; Mele, G. *Int. J. Mol. Sci.* **2011**, *12*, 5908.
3. Namera, A.; Nakamoto, A.; Saito, T.; Miyazaki, S. *J. Sep. Sci.* **2011**, *34*, 901.
4. Deng, Q. L.; Li, Y. L.; Zhang, L. H.; Zhang, Y. K. *Chin. Chem. Lett.* **2011**, *22*, 1351.
5. Andac, M.; Denizli, A. *RSC Adv.* **2014**, *4*, 31130.
6. Çulha, S.; Armutcu, C.; Uzun, L.; Şenel, S.; Denizli, A. *Mater. Sci. Eng. C.* **2015**, *52*, 315.
7. Ingavle, G. C.; Baillie, L. W. J.; Zheng, Y.; Lis, E. K.; Savina, I. N.; Howell, C. A.; Mikhalovsky, S. V.; Sandeman, S. R. *Biomaterials* **2015**, *50*, 140.
8. Dinu, M. V.; Ozmen, M. M.; Dragan, E. S.; Okay, O. *Polymer* **2007**, *48*, 195.
9. Andaç, M.; Baydemir, G.; Yavuz, H.; Denizli, A. *J. Mol. Recognit.* **2012**, *25*, 555.
10. Aydoğan, C.; Andaç, M.; Bayram, E.; Say, R.; Denizli, A. *Biotechnol. Progr.* **2012**, *28*, 459.
11. Baggiani, C.; Baravalle, P.; Giovannoli, C.; Anfossi, L.; Giraudi, G. *Anal. Bioanal. Chem.* **2010**, *397*, 815.
12. Baydemir, G.; Bereli, N.; Andaç, M.; Say, R.; Galaev, I. Y.; Denizli, A. *Colloids Surf. B Biointerfaces* **2009**, *68*, 33.
13. Bereli, N.; Andaç, M.; Baydemir, G.; Say, R.; Galaev, I. Y.; Denizli, A. *J. Chrom.* **2008**, *1190*, 18.
14. Koç, T.; Baydemir, G.; Bayram, E.; Yavuz, H.; Denizli, A. *J. Hazard. Mater.* **2011**, *192*, 1819.
15. Le Noir, M.; Plieva, F.; Hey, T.; Guieysse, B.; Mattiasson, B. *J. Chrom.* **2007**, *1154*, 158.
16. Huang, J. T.; Zhang, J.; Zhang, J. Q.; Zheng, S. H. *J. Appl. Polym. Sci.* **2005**, *95*, 358.
17. Lee, W. C.; Cheng, C. H.; Pan, H. H.; Chung, T. H.; Hwang, C. C. *Anal. Bioanal. Chem.* **2008**, *390*, 1101.
18. Kryscio, D. R.; Peppas, N. A. *Acta Biomater.* **2012**, *8*, 461.
19. Verheyen, E.; Schillemans, J. P.; van Wijk, M.; Demeniex, M. A.; Hennink, W. E.; van Nostrum, C. F. *Biomaterials* **2011**, *32*, 3008.
20. Fang, G.; Zhai, X.; Deng, Q.; Yuan, S.; Cao, M.; Wang, S. *Curr. Org. Chem.* **2012**, *16*, 1461.
21. Yang, K.; Zhang, L.; Liang, Z.; Zhang, Y. *Anal. Bioanal. Chem.* **2012**, *403*, 2173.
22. Turner, N. W.; Jeans, C. W.; Brain, K. R.; Allender, C. J.; Hlady, V.; Britt, D. W. *Biotechnol. Prog.* **2006**, *22*, 1474.
23. Bergmann, N. M.; Peppas, N. A. *Ind. Eng. Chem. Res.* **2008**, *47*, 9099.
24. He, H.; Fu, G.; Wang, Y.; Chai, Z.; Jiang, Y.; Chen, Z. *Biosens. Bioelectron.* **2010**, *26*, 760.
25. Ou, S. H.; Wu, M. C.; Chou, T. C.; Liu, C. C. *Anal. Chim. Acta.* **2004**, *504*, 163.
26. Svenson, J.; Andersson, H. S.; Piletsky, S. A.; Nicholls, I. A. *J. Mol. Recognit.* **1998**, *11*, 83.
27. Liu, Q.-Y.; QQ, G.; He, X.-W.; Li, W.-Y.; Chen, L.-X.; Zhang, Y.-K. *Chem. J. Chinese Univ.* **2008**, *29*, 505.
28. Gai, Q.; Qu, F.; Zhang, Y. *Sep. Sci. Technol.* **2010**, *45*, 2394.
29. Kashefi Mofrad, S. M. R.; Naeimpoor, F.; Hejazi, P.; Nematollahzadeh, A. *J. Appl. Polym. Sci.* **2015**, *132*, 3.
30. Haruki, M.; Konnai, Y.; Shimada, A.; Takeuchi, H. *Biotechnol. Prog.* **2007**, *23*, 1254.
31. Tov, O. Y.; Luvitch, S.; Bianco-Peled, H. *J. Sep. Sci.* **2010**, *33*, 1673.
32. Bergmann, N. M. Molecularly Imprinted Polyacrylamide Polymers and Copolymers with Specific Recognition for Serum Proteins; In Biomedical Engineering, The University of Texas: Austin, **2005**.
33. Rabieizadeh, M.; Kashefimofrad, S. M.; Naeimpoor, F. *J. Sep. Sci.* **2014**, *37*, 2983.
34. Derazshamshir, A.; Baydemir, G.; Andac, M.; Say, R.; Galaev, I. Y.; Denizli, A. *Macromol. Chem. Phys.* **2010**, *211*, 657.
35. Hua, Z.; Chen, Z.; Li, Y.; Zhao, M. *Langmuir* **2008**, *24*, 5773.
36. Simpson, N. J. K. Solid-Phase Extraction: Principles, Techniques, and Applications; CRC Press, New York, USA Taylor & Francis; ISBN: 1420056247: New York, USA **2000**.

37. Echlin, P. Handbook of Sample Preparation for Scanning Electron Microscopy and X-ray Microanalysis; Springer Science & Business Media; ISBN: 0387857311: New York, USA **2011**.
38. Michler, G. H. Electron Microscopy of Polymers; Springer Science & Business Media; ISBN: 3540363521: New York, USA **2008**.
39. Qin, L.; He, X. W.; Zhang, W.; Li, W. Y.; Zhang, Y. K. *Anal. Chem.* **2009**, *81*, 7206.
40. Bereli, N.; Saylan, Y.; Uzun, L.; Say, R.; Denizli, A. *Sep. Purif. Technol.* **2011**, *82*, 28.
41. Tamahkar, E.; Bereli, N.; Say, R.; Denizli, A. *J. Sep. Sci.* **2011**, *34*, 3433.
42. Liu, Q. Y.; Gai, Q. Q.; He, X. W.; Li, W. Y.; Chen, L. X.; Zhang, Y. K. *Gaodeng Xuexiao Huaxue Xuebao/Chem. J. Chinese Univ.* **2008**, *29*, 505.
43. Rouquerol, J.; Rouquerol, F.; Llewellyn, P.; Maurin, G.; Sing, K. S. Adsorption by Powders and Porous Solids: Principles, Methodology and Applications; Academic Press (Academic Press is an imprint of Elsevier); ISBN: 0080970362: **2013**.
44. Plieva, F. M.; Andersson, J.; Galaev, I. Y.; Mattiasson, B. *J. Sep. Sci.* **2004**, *27*, 828.